Static structure factor of dilute solutions of polydisperse fractal aggregates

Taco Nicolai, Dominique Durand, Jean-Christophe Gimel

Static structure factor of dilute solutions of polydisperse fractal aggregates

Taco Nicolai, Dominique Durand, and Jean-Christophe Gimel*
Laboratoire de Physico Chimie Macromoléculaire, URA CNRS, Université du Maine, 72017 Le Mans Cedex, France
(Received 25 July 1994)

We have calculated the z-average static structure factor $[S(q)_z]$, z-average radius of gyration (R_{gz}), and the weight average aggregation number (m_w) of fractal aggregates with an aggregate number distribution given by $N(m) \propto m^{-\tau} f(m/m^*)$. Here, q is the scattering wave vector and for the cutoff function $f(m/m^*)$ at a characteristic aggregation number m^* we have chosen a stretched exponential function. We derive expressions for the prefactors of the scaling relations $m_w \propto R_{gz}^{df^*}$ and $S(q)_z \propto (qR_{gz})^{-df^*}$ and make explicit the conditions for their validity at finite values of m_w and qR_{gz}. For values of τ close to two these conditions are shown to be very difficult to meet in practice. For the case of aggregates formed by a percolation process where $\tau = 2.2$ it is shown that attempts to measure df^* directly from the slope of $\log_{10}(m_w)$ vs $\log_{10}(R_{gz})$ or $\log_{10}(S(q)_z)$ vs $\log_{10}(q)$ are biased by the effect of the internal and/or external cutoff of the fractal regime.

INTRODUCTION

Particle growth by random aggregation often leads to the formation of broad distributions of self-similar particles and in some cases the system eventually forms a gel. Some examples are aggregation of gold colloids,[1] silica colloids[2] or globular proteins;[3] polycondensation of triol and diisocyanate[4] or epoxy and diamine;[5] polyaddition of MMA and EGDMA,[6] or styrene and divinylbenzene.[7]

The aggregation process in dilute solutions has been studied intensively both theoretically using the Smoluchowski equation and by computer simulation.[8] From this work it was concluded that many aggregation processes lead to the formation of self-similar particles with the following aggregation number distribution:

$$N(m) \propto m^{-\tau} f(m/m^*), \quad m^* \gg 1 \; . \tag{1}$$

$f(x)$ is a function decreasing faster than any power law which cuts off the distribution at an aggregation number m^*. Well known examples are diffusion limited (DLCA) and reaction limited cluster aggregation (RLCA). Aggregates formed by DLCA have a fractal dimension $df = 1.8$ and the size distribution is characterized by $\tau = 0$, while for RLCA $df = 2.1$ and $\tau = 1.5$. For a number of model systems these results have been experimentally verified. At higher concentrations collisions between aggregates can no longer be considered independent, and the Smoluchowski equation cannot be applied. It has been proposed that the growth of aggregates that fill up the whole space can be described by percolation theory.[9] Computer simulations of percolation show that self-similar aggregates are formed with $df = 2.5$ and a size distribution characterized by $\tau = 2.2$.[10] A lot of experimental work which aimed at checking these predictions is reported in the literature, see, e.g., Refs. 4–7 and 11. Few computer simulations have been done covering intermediate concentrations and little is known about the structure and size distribution of the aggregates formed in the transition zone. We have recently conducted Monte-Carlo calculations showing the transition from an initial growth by DLCA to a percolation process just before reaching the gel point.[12]

Experimentally df can be measured using scattering techniques, while τ can be obtained from size exclusion chromatography or dynamic light scattering. Two independent relations can be used to determine df:

$$m_w \propto R_{gz}^{df^*}, \quad m_w \gg 1 \tag{2}$$

or

$$I(q) \propto q^{-df^*}, \quad qR_{gz} \gg 1, \quad \text{and } qr_0 \ll 1 \; . \tag{3}$$

Here m_W is the weight average aggregation number, R_{gz} is the z-average radius of gyration, r_0 is the radius of the elementary unit, and $I(q)$ is the scattered light intensity. $q = (4\pi/\lambda)\sin(\theta/2)$ is the scattering wave vector with λ the wavelength of the incident beam in the sample and θ the scattering angle. df^* is an apparent fractal dimension equal to the true fractal dimension if $\tau < 2$ and $df^* = df(3-\tau)$ if $2 < \tau < 3$. This difference can be exploited to obtain τ if $\tau > 2$ by measuring both the polydisperse sample and a monodisperse fraction. It is not always trivial, however, to do the measurements under the right conditions stated in Eqs. (2) and (3) due to the limited experimentally accessible q range which also limits the maximum R_{gz} that can be measured. It is therefore important to establish the deviations from the limiting behavior as a function of m_w, qr_0, and qR_{gz}. One of the objects of this study is to determine these deviations and to evaluate the validity of experimental results reported in literature. It will be shown that for systems with size distributions characterized by values of τ close to two, df^* can be determined accurately only at very large values of m_W or qR_{gz}. Aggregation by percolation, with $\tau = 2.2$, is an important example of such a system and much attention will be given to this case. We will show that for most, if not all, experimental determinations of df^* which aimed at verifying the percolation

0163-1829/94/50(22)/16357(7)/$06.00

theory, the conditions for the correct use of Eqs. (2) and (3) were not fulfilled.

NUMERICAL CALCULATIONS

To calculate explicitly the dependence of m_W on R_{gz} we have to assume a specific form for the cutoff function in Eq. (1). Usually one takes an exponential decay which is also expected theoretically for a number of aggregation processes. Here, we will use a stretched exponential so that we can evaluate the effect of a faster or slower decaying cutoff function. The aggregation number distribution used in the simulations is thus given by

$$N(m) \propto m^{-\tau} \exp[-(m/m^*)^{\beta}], \quad m^* \gg 1 \ . \tag{4}$$

Since most fractal systems have a fractal dimension around two, we will first show the results for $df=2$ and $\beta=1$ and discuss the influence of changing df and β subsequently. The weight average aggregation number and the z-average radius of gyration are given by

$$m_w = \frac{\sum_{m=1}^{\infty} m^2 N(m)}{\sum_{m=1}^{\infty} m \cdot N(m)} \ , \tag{5}$$

$$R_{gz} = \left[\frac{\sum_{m=1}^{\infty} m^2 N(m) R_g^2}{\sum_{m=1}^{\infty} m^2 N(m)} \right]^{0.5} \tag{6a}$$

with

$$m = a R_g^{df} \tag{6b}$$

where a is a constant which depends on the structure of the aggregates see below. As we consider only systems with $m^* \gg 1$, the deviation of the scaling relations (4) and (6b) are negligible. Using Eq. (3) in Eq. (5) and assuming $m^* \gg 1$ one obtains for m_W

$$\begin{aligned} m_w &= \frac{\Gamma[(3-\tau)/\beta]}{\Gamma[(2-\tau)/\beta]} m^*, \quad \tau < 2 \\ m_w &= \frac{\Gamma(1/\beta) m^*}{\beta \ln(m^*) - \kappa}, \quad \tau = 2 \\ m_w &= \frac{(\tau-2)}{\beta} \Gamma\left[\frac{3-\tau}{\beta}\right] m^{*(3-\tau)}, \quad 2 < \tau < \min(2+\beta, 3) \end{aligned} \tag{7}$$

with $\Gamma(x)$ the gamma function and κ the Euler constant ($\kappa = 0.577$), R_{gz} is related to m^* as follows:

$$m^* = a \left[\frac{\Gamma[(3-\tau)/\beta]}{\Gamma[(3+2/df-\tau)/\beta]} \right]^{df/2} R_{gz}^{df}, \quad \tau < 3 \ . \tag{8}$$

In Fig. 1, m_w is plotted as a function of R_{gz} for values of τ between 0 and 2.3. The graph shows that the limiting slope changes for $\tau > 2$ and is approached very slowly for values of τ close to two. The slope, $\delta \log_{10}(m_w)/\delta \log_{10}(R_{gz})$, is shown in Fig. 2(a) as a function of m_w and the deviation of the final slope is plotted in Fig. 2(b). It is clear that at a fixed value of m_W the deviation is largest around $\tau=2$. To illustrate the strong τ dependence, we have plotted in Fig. 2(c) the value of m_w needed to approach the final slope within 5% ($m_w^{5\%}$) as a function of τ. In real systems, however, a is not a constant for small values of m, but depends on the structure and the flexibility of the elementary units which means that in practice the deviation at small m_W is less obvious.

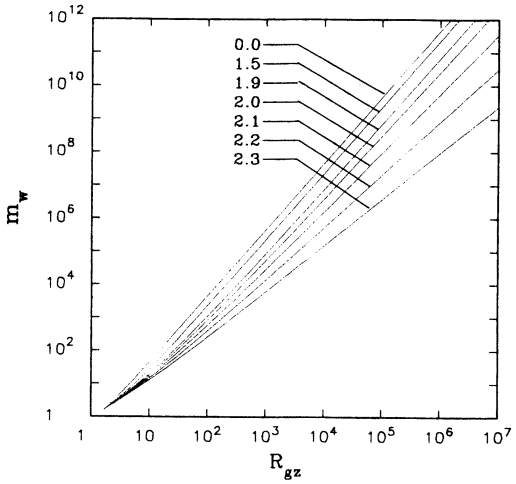

FIG. 1. Double logarithmic plot of the weight average aggregation number versus the z-average radius of gyration of aggregates with $df=2$, $\gamma=1$, and $\beta=1$ at different values of the polydispersity exponent, τ, as indicated in the graph.

The intensity of the light scattered by a dilute solution of monodisperse aggregates is related to the static structure factor $[S(q)]$ of the aggregates: $I(q)/C \propto mS(q)$, where C is the monomer concentration. For isotropic systems in three dimensions the structure factor is related to the pair-correlation function $[g(r)]$ in the following way:[13]

$$S(q) = \frac{P(q)}{m} \left[1 + 4\pi \int_0^{\infty} g(r) r^2 \frac{\sin(qr)}{qr} dr \right] , \tag{9}$$

where $P(q)$ is the form factor of the elementary unit (monomer) of the aggregates. Here, $S(q)$ is defined, as usual, such that $S(q=0)=1$ contrary to the definition used in Ref. 13 where $S(q=0)=m$. We will assume that the number of monomers, $N(r)$, which lie in a sphere of radius r centered on an arbitrary monomer is given by $N(r)=(r/r_0^*)^{df}$ for $r_0^* \ll r \ll \xi$. r_0^* is equal to the monomer radius only if we ignore the influence of short-range excluded volume interactions. In reality r_0^* depends on the local structure of the aggregates, but is of the same order of magnitude. In the calculations we have taken $r_0^* = r_0$ as the unit length. Using this expression for $N(r)$, the pair-correlation function of the aggregate can be written as

$$g(r) = \frac{df}{4\pi r_0^{*df}} r^{df-3} f(r/\xi), \quad r \gg r_0^* \ , \tag{10}$$

where $f(r/\xi)$ is a cutoff function introduced to take into

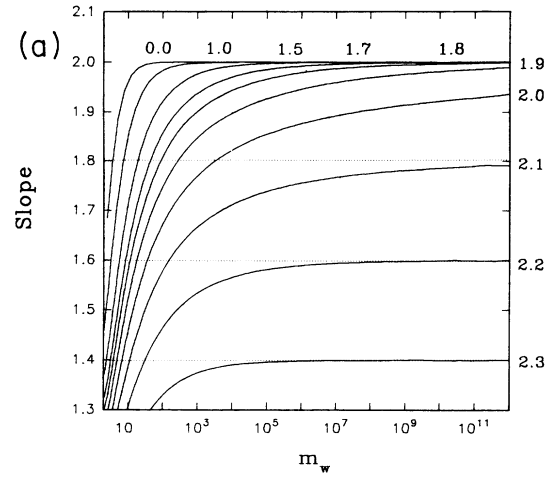

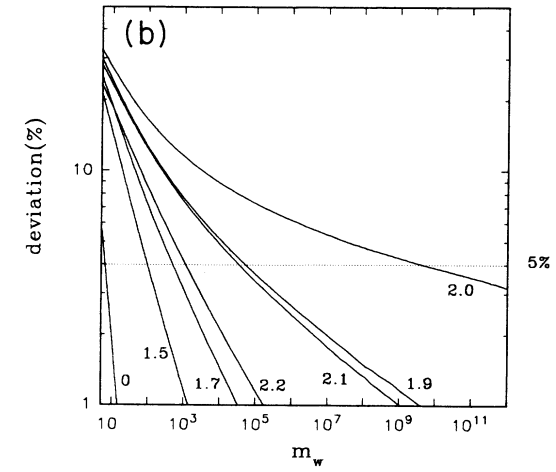

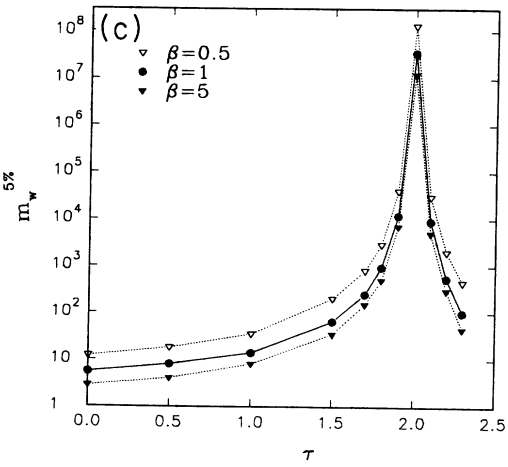

FIG. 2. (a) Semilogarithmic plot of the slope of the curves in Fig. 1 as a function of the weight average aggregation number at different values of the polydispersity exponent, τ, as indicated in the graph. (b) Double logarithmic plot of the percentage deviation of the slope from the limiting value versus the weight average aggregation number at different values of the polydispersity exponent, τ, as indicated in the graph. (c) Double logarithmic plot of the weight average aggregation number where the deviation of the slope from its limiting value is 5% versus the polydispersity exponent at three values of the exponent β, see text.

account the finite size (ξ) of the fractal. $f(r/\xi)$ is close to unity for $r<\xi$ and decreases faster than any power law to zero for $r>\xi$. We will again assume a stretched exponential form: $f(r/\xi)=\exp[-(r/\xi)^{\gamma}]$ so that by varying γ we can evaluate the influence of the sharpness of the cutoff function. At small values of r, $g(r)$ is determined by the local structure of the aggregates. The influence of local excluded volume effects modifies the shape of $S(q)$ for values of qr_0 around unity.[14,15] Here, we will not consider these effects, but assume that Eq. (10) is valid down to $r=r_0^*$. Normalizing $g(r)$ such that $4\pi\int g(r)r^2dr=m-1$, one obtains

$$S(q)=\frac{P(q)}{m}\left[1+\frac{df}{r_0^{*df}}\int_{r_0^*}^{\infty}r^{df-1}\exp[-(r/\xi)^{\gamma}]\times\frac{\sin(qr)}{qr}dr\right]. \tag{11}$$

In the special case when $\gamma=1$, Eq. (10) can be solved analytically for $\xi\gg r_0^*$:[13,16]

$$S(q)=\frac{P(q)}{m}\left[1+\frac{1}{(qr_0^*)^{df}}\frac{df\Gamma(df-1)}{(1+1/q^2\xi^2)^{(df-1)/2}}\times\sin[(df-1)tg^{-1}(q\xi)]\right]. \tag{12}$$

In general, for any value of γ, in the limit of $q\xi\gg1$ we have

$$S(q)=\frac{b}{m}q^{-df},\quad r_0^*\ll q^{-1}\ll\xi \tag{13}$$

with

$$b=r_0^{*-df}df\Gamma(df-1)\sin\left[\frac{\pi}{2}(df-1)\right].$$

As expected, b in Eq. (13) is independent of the overall size of the aggregate, i.e., b does not depend on ξ or γ.

Using $g(r)$ as defined by Eq. (10) we can calculate the prefactor a in Eq. (6b). The radius of gyration is given by $R_g^2=4\pi\int g(r)r^4dr/2m$ so that

$$m=\left[\frac{\xi}{r_0^*}\right]^{df}\frac{df\Gamma(df/\gamma)}{\gamma},\quad m\gg1 \tag{14}$$

and

$$R_g^{2=}\xi^2\frac{\Gamma[(df+2)/\gamma]}{2\Gamma(df/\gamma)},\quad R_g\gg r_0^*. \tag{15}$$

Combining Eqs. (14) and (15) we obtain

$$a=\left[\frac{2\Gamma(df/\gamma)}{\Gamma[(df+2)/\gamma]}\right]^{df/2}\frac{df\Gamma(df/\gamma)}{\gamma r_0^{*df}}. \tag{16}$$

It follows from Eqs. (6b) and (13) that

$$S(q)=\frac{b}{a}(qR_g)^{-df},\quad r_0^*\ll q^{-1}\ll R_g. \tag{17}$$

The prefactor b/a is independent of the local structure of the aggregate, i.e., r_0^*.

If we want to include the effect of polydispersity, we need to calculate the z-average static structure factor as

$$S(q)_z = \frac{\sum_{m=1}^{\infty} m^2 N(m) S(q)}{\sum_{m=1}^{\infty} m^2 N(m)} . \quad (18)$$

The parameter b is not influenced by polydispersity, so that

$$S(q)_z = \frac{b}{a_z} (qR_{gz})^{df^*} , \quad (19)$$

where a_z is the prefactor in relation (2) and is given by Eqs. (7) and (8).

We consider again first the case $df = 2$, $\beta = 1$ and $\gamma = 1$ and evaluate the influence of these parameters subsequently. $S(q)_z$ is plotted in Fig. 3 for values of τ between 0 and 2.3. The graph shows again that the limiting slope changes for $\tau > 2$ and is approached very slowly for values of τ close to two. The slope, $\delta \log_{10}(S(q)_z)/\delta \log_{10}(qR_{gz})$, is shown in Fig. 4(a) as a function of qR_{gz} and the deviation of the final slope is plotted in Fig. 4(b). The value of qR_{gz} needed to approach the final slope within 5% ($qR_{gz}^{5\%}$) are shown in Fig. 4(c).

Influence of the cutoff function of $N(m)$ at large m

The influence of the shape of the cutoff function of $N(m)$ can be evaluated by varying β in Eq. (3) keeping $df = 2$ and $\gamma = 1$. Figures 2(c) and 4(c) show that if the cutoff is sharper (larger β), the values of R_{gz} and qR_{gz} needed to approach to the final slope are smaller.

Influence of the fractal dimension

Varying the fractal dimension keeping $\beta = 1$ and $\gamma = 1$ leads, of course, to different final slopes in Fig. 1, but

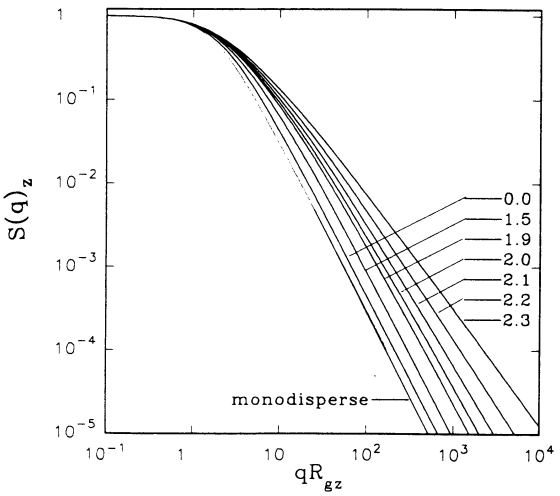

FIG. 3. Double logarithmic plot of the z-average structure factor versus qR_{gz} of aggregates with $df = 2, \gamma = 1$ and $\beta = 1$ at different values of the polydispersity exponent, τ, as indicated in the graph.

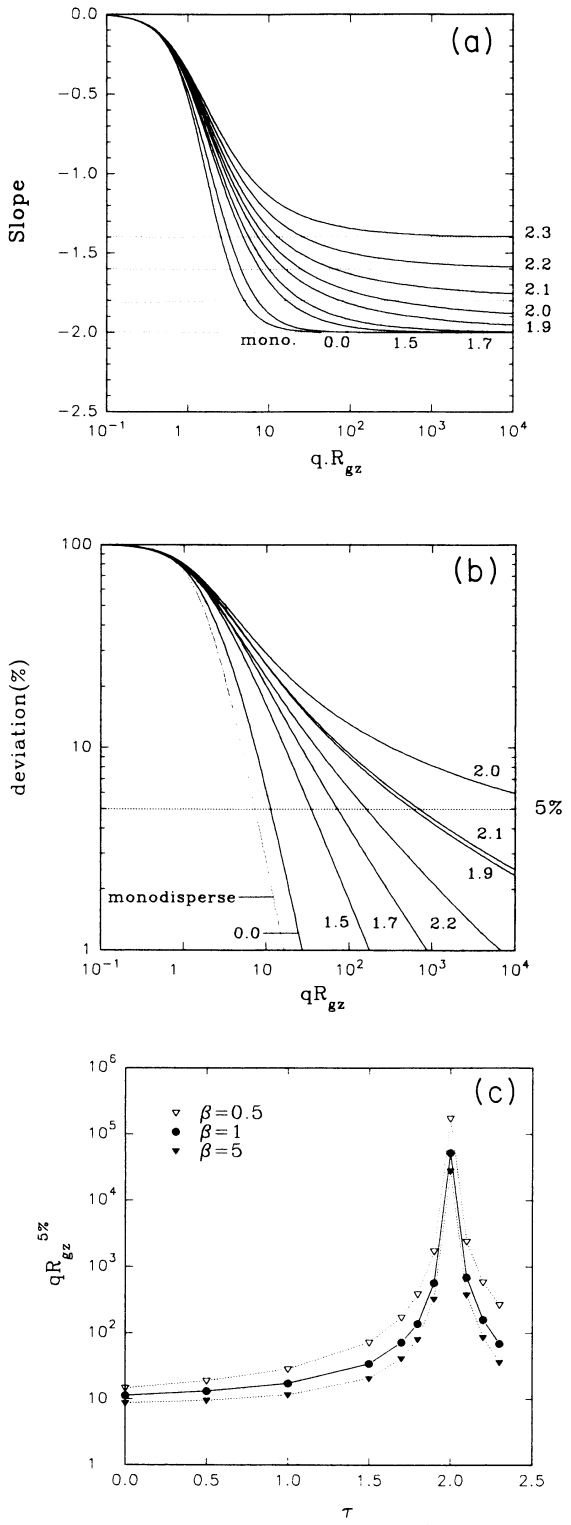

FIG. 4. (a) Semilogarithmic plot of the slope of the curves in Fig. 3 as a function of qR_{gz} at different values of the polydispersity exponent, τ, as indicated in the graph. (b) Double logarithmic plot of the percentage deviation of the slope from the limiting value versus qR_{gz} at different values of the polydispersity exponent, τ, as indicated in the graph. (c) Double logarithmic plot of the qR_{gz} value where the deviation of the slope from its limiting value is 5% ($qR_{gz}^{5\%}$) versus the polydisperity exponent at three values of the exponent β, see text.

$\delta \log_{10}(m_w)/\delta \log_{10}(R_{gz})$ shows the same deviations from the final slope when plotted as a function of m_w. This means, however, that the deviations at fixed R_{gz} increase with decreasing df.

The static structure factor for monodisperse fractals is shown in Fig. 5(a) at various values of df while keeping $\gamma=1$. When df approaches 3 closely the initial slope of $\log_{10}[S(q)]$ vs $\log_{10}(qR_g)$ is 4 as expected for dense objects and only reaches df at larger qR_g. At $df=3$ the slope remains 4. The final slope is approached at smaller qR_{gz} if df is increased. This is illustrated in Fig. 5(b), where $qR_{gz}^{5\%}$ is plotted as a function of τ for three values of df with $\beta=1$ and $\gamma=1$.

Influence of the cutoff function of $g(r)$ at large r

The influence of shape of the cutoff function of $g(r)$ can be evaluated by calculating numerically $S(q)$ using Eq. (11). The influence of γ is illustrated for monodisperse fractals in Fig. 6(a). For large values of γ undulations appear due to the sharpening of the interface. If we combine $df=3$ with $\gamma=\infty$ we obtain the static structure factor of a sphere. The effect of the undulations is already important for $\gamma=2$ where the slope reaches a maximum value 2.37 at $qR_g=4$. The static structure factor of ideal chains (the so-called Debye function) seems well described by Eq. (11) with $\gamma\approx 1.3$. Polydispersity reduces the amplitude of these undulations. The final slope is reached more quickly at larger values of γ as illustrated in Fig. 6(b), where $qR_{gz}^{5\%}$ is plotted as a function of τ for three values of γ, $df=2$, and $\beta=1$.

Again $\delta \log_{10}(m_W)/\delta \log_{10}(R_{gz})$ shows the same deviations from the final slope when plotted as a function of m_w. From Eqs. (7), (8), and (16) it follows that the deviations at fixed R_{gz} increase weakly with decreasing γ.

Influence of the local structure

In the previous calculations we have used $qr_0 \ll 1$. If we assume $P(q)=1$ and $qR_{gz} \gg 1$, the deviation of the

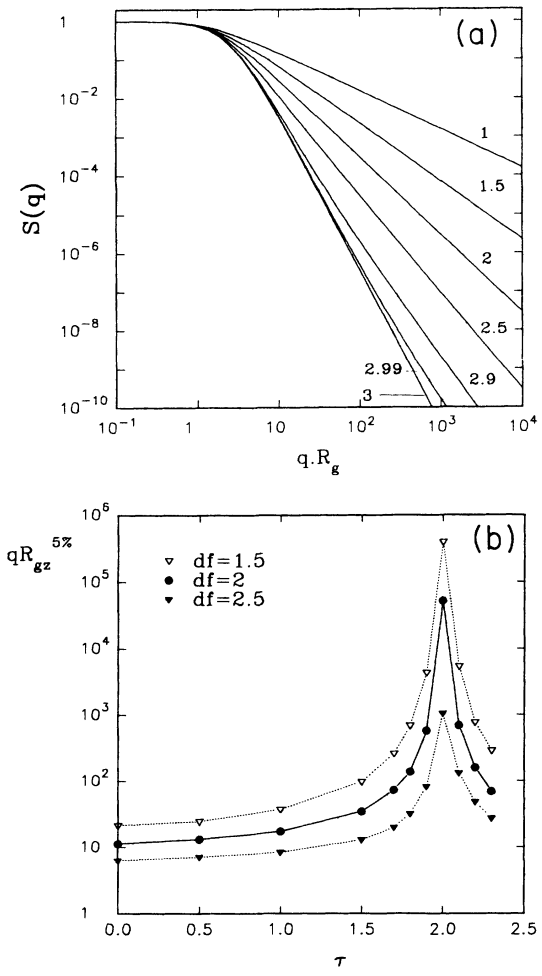

FIG. 5. Double logarithmic plot of the structure factor versus qR_g of monodisperse aggregates with $\gamma=1$ at different values of the fractal dimension as indicated in the graph. (b) Double logarithmic plot of the qR_{gz} value where the deviation of the slope from its limiting value is 5% ($qR_{gz}^{5\%}$) versus the polydispersity exponent at three values of the fractal dimension with $\beta=1$ and $\gamma=1$.

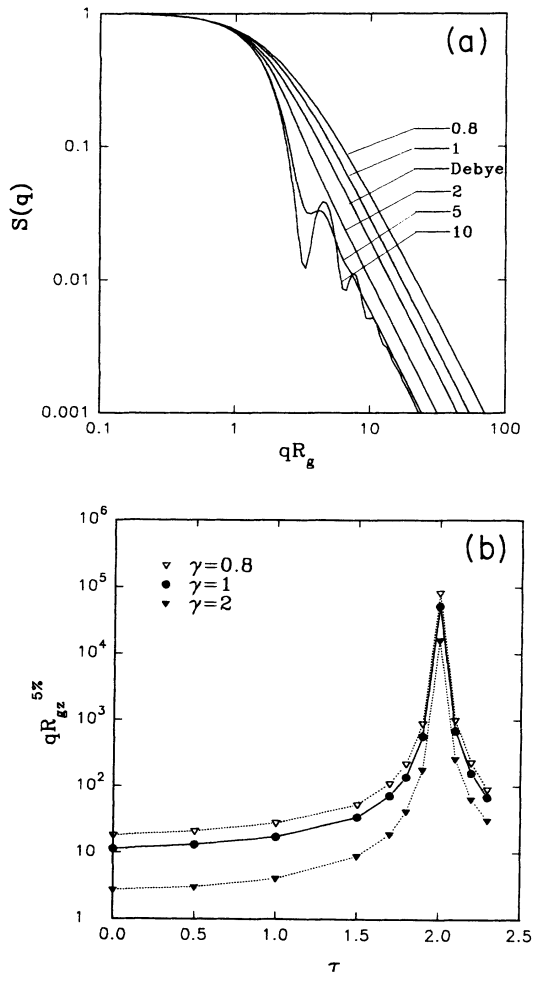

FIG. 6. (a) Double logarithmic plot of the structure factor versus qR_g of monodisperse aggregates with $df=2$ at different values of the exponent γ, as indicated in the graph. (b) Double logarithmic plot of the qR_{gz} values where the deviation of the slope from its limiting value is 5% ($qR_{gz}^{5\%}$) versus the polydispersity exponent at three values of the exponent γ with $df=2$ and $\beta=1$.

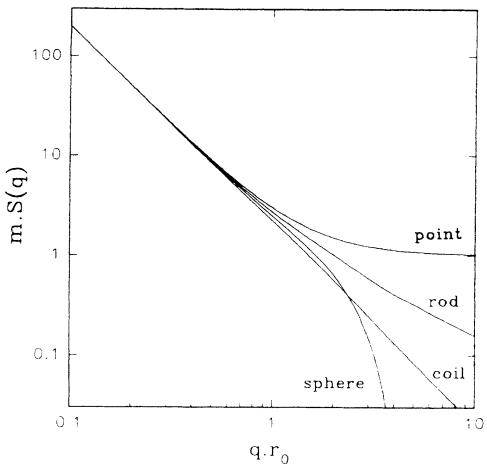

FIG. 7. Double logarithmic plot of the structure factor of monodisperse aggregate with $df=2$, and $\gamma=1$ for different form factors of the elementary unit as a function of qr_0.

fractal slope with increasing qr_0 is less than 5% for qr_0 smaller than about 0.3. Here we did not take into account short-range excluded volume interactions. Hasmy *et al.*[14] have done computer simulations to see the influence of short-range excluded volume interactions. They find that, still, for $qr_0<0.3$ the deviation from the fractal slope becomes small. Of course, in real systems the elementary unit is not a point scatterer and $S(q)$ is modified by the static structure factor of the elementary unit. In Fig. 7 we have plotted $S(q)$ vs qr_0 using for $P(q)$ the static structure factor of a sphere, rod, and ideal coil with r_0 the radius of the sphere, half the rod length, and the radius of gyration of the coil, respectively. It is clear that in practice the deviation at $qr_0>0.3$ will be less obvious especially if the elementary unit is itself fractal with a fractal dimension close to that of the aggregate. In these plots we have ignored the effect of short-range exclude volume effects which modify the shape of $S(q)$ around $qr_0=1$.

DISCUSSION

In order to apply the results of the calculations to real systems we need to know the values of β and γ for the particular system. For a large number of aggregation processes described by the Smoluchowski equation such as, DLCA and RLCA, the cutoff function is close to a single exponential ($\beta=1$), and for the percolating clusters it can be approximated by a stretched exponential with $\beta\approx 0.9$.[17] No theoretical expression of the cutoff function of $g(r)$ is known. However, Klein *et al.*[12] have calculated the structure factor of simulated aggregates formed by DLCA and RLCA. The results were well described by the empirical relation

$$S(qR_g)=\left[1+\sum_{s=1}^{4} c_s(qR_g)^{2s}\right]^{-df/8}, \tag{20}$$

with df equal to 1.8 and 2.1 for DLCA and RLCA, respectively, and c_s coefficients which depend on the aggregation process. c_1 is determined by the Guinier expansion and c_4 is determined by the prefactor, b/a in Eq. (17). If we compare these results with Eq. (9) we find a close agreement if $\gamma=2$ as shown in Fig. 8. The pair-correlation function of simulated aggregates formed by percolation also shows a stretched exponential cutoff with $\gamma\approx 2$.[12] Whether $\gamma=2$ and $\beta=1$ are reasonable estimates even in other types of aggregations has to be established experimentally. In principle, one could apply the equations given in the previous section to fit directly $S(q)_z$ with df, τ, β, and γ floating parameters. In practice, however, the experimental data are not accurate enough to make such an analysis useful. A better approach is to fix some parameters based on prior knowledge in order to obtain precise values of the floating parameters. For example one could determine df and γ by fitting $S(q)$ of monodisperse fractions and fix these parameters in the fit of the polydisperse sample. Alternatively, one could measure τ from size exclusion chromatography or dynamic light scattering. Fitting R_{gz} as a function of m_w directly is often complicated by the uncertainty in the size and molar mass of the elementary unit. In addition, in many cases the elementary unit is not monodisperse.

Although one should try to fit $S(q)_z$ and R_{gz} directly, it is of practical interest to establish the conditions for the application of Eqs. (2) and (3). Unless one uses special optical equipment, it is difficult to perform light-scattering measurements at an angle of observation below 5° so that $25<q^{-1}<700$ nm. The limits may vary somewhat depending on the wavelength of the incident light and the refractive index of the solution, but in general the experimental q range is not much broader. In practice, for an accurate measurement of the slope one needs to measure it over at least half a decade which means that

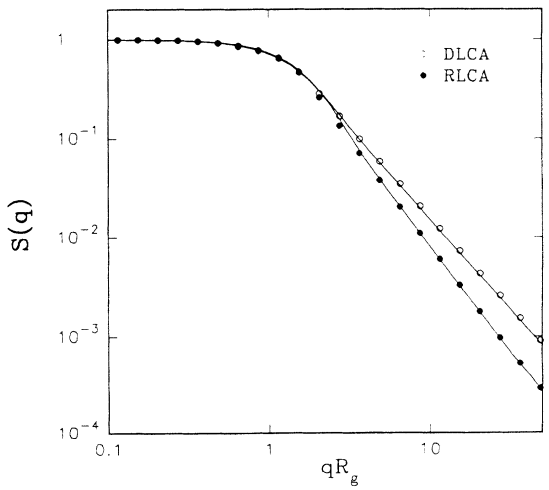

FIG. 8. Double logarithmic plot of the structure factor versus qR_g of monodisperse aggregates formed by DLCA and RLCA. The symbols represent the result of simulations by Klein *et al.* (Ref. 1) and the solid lines give the calculated results using Eq. (11) with $df=1.8$ and $\gamma=2$ for DLCA and $df=2.1$ and $\gamma=2$ for RLCA.

the slope can be measured in the range $45 < q^{-1} < 400$ nm. This means that in order to measure the fractal dimension within 5% by light scattering, we need $R_{gz} > 45(qR_{gz}^{5\%})$. For a dilute solution of aggregates formed by percolation ($\beta=1$, $\gamma=2$, $\tau=2.2$, and $df=2.0$) we have found $qR_{gz}^{5\%}=65$ so that we need $R_{gz} > 3000r_0^*$. In most real systems $r_0^* > 1$ nm so that we need $R_{gz} > 3$ μm. In x-ray- or neutron-scattering experiments the limiting factor for an accurate measurement of the fractal dimension is the size of the elementary unit. For a measurement within 5% we need both $qR_{gz} > qR_{gz}^{5\%}$ and $qr_0^* < 0.3$. For the case of percolation this means that we need $R_{gz} > 210r_0^*$. To apply Eq. (2) we need to measure R_{gz} and m_w and measure the slope of $\log_{10}(m_w)$ versus $\log_{10}(R_{gz})$ over at least half a decade. For the case of percolation we have found $m_w^{5\%}=500$ which means that for a measurement of df within 5% we need $m_w > 900$. The corresponding R_{gz} value can be calculated using $m_w = a_z R_{gz}^{df*}$ for $m_w \gg m$ with a_z given by combining Eqs. (7), (8), and (16). If $\beta=1$, $\gamma=2$, $\tau=2.2$, and $df=2.0$, then $a_z=2.23$ so that $m_w > 900$ implies $R_{gz} > 67r_0^*$.

A look at the literature shows us that many authors have applied Eqs. (2) and (3) without proper consideration of the constraints. An example of a reportedly very polydisperse system is a solution of aggregates formed by slow aggregation of colloidal silica studied by Martin.[18] He reported that for this system the number distribution can be described by Eq. (1) with $\tau=1.9$ and $\beta=1$. The fractal dimension $df=2.05$ was measured in the range $30 < q^{-1} < 400$ nm. Assuming $\gamma=2$ we can read from Fig. 6(b) that $qR_{gz}^{5\%} \approx 140$. The size of the elementary unit is 7 nm so that for an error in df less than 5%, R_{gz} must have been larger than 0.15 mm, which is unlikely. In general, aggregation in dilute conditions leads to much less polydisperse samples so that Eq. (3) can be applied without the need of extremely large values of R_{gz}.

When the aggregates are formed by a percolation process, however, the polydispersity is high and from the previous discussion it is clear that the constraints for the correct application of Eq. (3) are severe. It is therefore not surprising that in most if not all such studies either the condition $qR_{gz} > qR_{gz}^{5\%}$ or $qr_0^* < 0.3$ are not met. In some cases both these conditions are not met in the q range over which the slope was measured, which might lead to compensatory effects. An additional complication is that it is not always clear what should count as the elementary unit. The constraints for the application of Eq. (2) are less stringent provided that r_0^* is not too large, but still most applications of Eq. (2) to percolating systems reported in the literature were not unambiguously done at sufficiently large m_w and R_{gz}.

CONCLUSIONS

The structure and size distribution can be expressed in terms of four parameters: df, γ, τ, and β.

The prefactors occurring in the scaling relations: $m_w \propto R_{gz}^{df*}$ and $S(q)_z \propto (qR_{gz})^{-df*}$, can be written in terms of these four parameters.

We have established that the apparent fractal dimension of systems with a polydispersity exponent close to two can, in practice, not be directly obtained from the slope of $\log_{10}[S(q)_z]$ vs $\log_{10}(qR_{gz})$ or $\log_{10}(m_w)$ vs $\log_{10}(R_{gz})$. An inspection of the literature showed that attempts to establish df^* in this way for the case of percolating systems were probably biased by the effect of the internal and/or external cutoff of the fractal regime.

In order to determine the parameters that characterize the structure (df and γ) and the size distribution (τ and β) of the aggregates it is necessary to fit $\log_{10}[S(q)_z]$ vs $\log_{10}(qR_{gz})$ or $\log_{10}(m_w)$ vs $\log_{10}(R_{gz})$ directly to the equations given above.

*Present address: Department of Physical Chemistry, University of Uppsala, Box 532, 751 21 Uppsala, Sweden.

[1]R. Klein, D. A. Weitz, M. Y. Lin, H. M. Lindsay, R. C. Ball, and P. Meakin, Progr. Colloid Polym. Sci. **81**, 161 (1990).

[2]G. Dietler, C. Aubert, D. S. Cannell, and P. Wiltzius, Phys. Rev. Lett. **57**, 3117 (1986).

[3]J. C. Gimel, D. Durand, and T. Nicolai, Macromolecules **27**, 583 (1994).

[4]M. Adam, D. Lairez, F. Boué, J. P. Busnel, D. Durand, and T. Nicolai, Phys. Rev. Lett. **67**, 3456 (1991); M. Adam, M. Delsanti, J. P. Munch, and D. Durand, J. Phys. (Paris) **48**, 1809 (1987); E. Bouchaud, M. Delsanti, M. Adam, M. Daoud, and D. Durand, J. Phys. (Paris) **47**, 1273 (1986).

[5]W.-L. Wu, B. J. Bauer, and W. Su, Polymer **30**, 1384 (1989).

[6]L. Fang, W. Brown, and C. Konak, Macromolecules **24**, 6839 (1991).

[7]L. Leibler and F. Schosseler, Phys. Rev. Lett. **55**, 1110 (1985); F. Schosseler, M. Daoud, and L. Leibler, J. Phys. (Paris) **51**, 2373 (1990).

[8]T. Vicsek, *Fractal Growth Phenomena* (World Scientific, London, 1989).

[9]P. G. de Gennes, *Scaling Concept in Polymer Physics* (Cornell University Press, London, 1979).

[10]D. Stauffer and A. Aharony, *Introduction to Percolation Theory*, 2nd. ed. (Taylor & Francis, London, 1992).

[11]J. Bauer, P. Lang, W. Burchard, and M. Bauer, Macromolecules **24**, 2634 (1991); E. V. Patton, J. A. Wesson, M. Rubinstein, J. C. Wilson, and E. Oppenheimer, Macromolecules **22**, 1946 (1989).

[12]J. C. Gimel, D. Durand, and T. Nicolai (unpublished).

[13]J. Teixeira, in *On Growth and Form*, edited by H. E. Stanley and N. Ostrowsky (Martinus Nijhoff, Dordrecht, 1986), p. 145.

[14]A. Hasmy, M. Foret, J. Pelous, and R. Jullien, Phys. Rev. B **48**, 9345 (1993).

[15]P. Dimon, S. K. Sinha, D. A. Weitz, C. R. Safinya, G. S. Smith, W. A. Varady, and H. M. Lindsay, Phys. Rev. Lett. **57**, 595 (1986).

[16]T. Freltoft, J. K. Kjems, and S. K. Sinha, Phys. Rev. B **33**, 269 (1986).

[17]D. Stauffer, in *On Growth and Form* (Ref. 13), p. 79; P. L. Leath, Phys. Rev. B **14**, 5046 (1976).

[18]J. E. Martin, Phys. Rev. A **36**, 3415 (1987).